

Organically Modified Aluminum Phosphates: Synthesis and Characterization of Model Compounds Containing Diphenyl Phosphate Ligands

Zbigniew Florjańczyk,* Anna Lasota, Andrzej Wolak, and Janusz Zachara

Faculty of Chemistry, Warsaw University of Technology, ul. Noakowskiego 3, 00-664 Warszawa, Poland

Received December 2, 2005. Revised Manuscript Received February 6, 2006

Reactions of diphenylphosphoric acid (DPPA) with AlMe_3 , AlEt_3 , $\text{Al}(\text{tBu})_3$, and boehmite have been studied. The reaction with $\text{Al}(\text{tBu})_3$ yields the molecular complex $([\text{Al}(\text{tBu})_2\text{AlO}_2\text{P}(\text{OPh})_2]_2)$ (**1**), which in the solid state exists as a centrosymmetric dimer consisting of two four-coordinate Al centers linked by diphenyl phosphate (DPP) bridges. The ligand bite distance $\text{Al}\cdots\text{Al}$ in **1** is equal to 4.75 Å. Reactions with AlMe_3 or AlEt_3 lead to polymeric aluminum organophosphates $(\{\text{Al}[\text{O}_2\text{P}(\text{OC}_6\text{H}_5)_2]_3\}_n)$ (**2**). These polymers were characterized by elemental analysis, in addition to XRD, TGA, FT-IR, SEM, and MAS NMR techniques. The results of MAS NMR and FT-IR studies have shown that $\text{Al}(\text{OP})_6$ units are the basic chain building blocks that produce condensed structures. The same type of Al environment was observed in aluminophosphate phase found in the products of the reaction with boehmite. This phase reveals a fibrous structure attributed to the close-packed hexagonal columnar structure consisting of polymeric chains of catena- $\text{Al}(\text{DPP})_3$ with the unit cell parameters $a = 15.14(4)$ Å and $c = 14.44(3)$ Å ($V = 2870$ Å³). The number of molecules in the crystallographic unit (Z) is 3. According to this model the mean diameter of the chain is equal to the parameter a (15.14 Å) while the distance between adjacent Al atoms linked by three phosphate bridges can be estimated as $c/3 = 4.81$ Å. The latter value matches perfectly the value of the $\text{Al}\cdots\text{Al}$ distance determined for compound **1**.

Introduction

The large number of hybrid macromolecules that contain inorganic elements in the polymer backbone and organic side groups constitutes an important area of material chemistry. Most inorganic–organic hybrid materials are prepared either by incorporation of organic moieties into organized inorganic structures or by condensation of low-molecular precursors. The modification of silica or titanium oxide fillers by organosilane coupling agents and the sol–gel technology involving the hydrolysis of organo-silicates, -titanates, or -aluminates to multihydroxy compounds which then condense into three-dimensional structures are classical examples of this.

Within the domain of aluminum-containing materials the main interest has been focused on organoclay hybrids prepared by introducing hydrophobic organic cations into layered aluminosilicates, which allows the formation of nanocomposites with various types of organic polymers.^{1–5} There have also been several attempts to incorporate organophosphonic and organophosphoric moieties into aluminophosphonate and aluminophosphate structures, respectively. As a result, new types of materials such as porous organic–inorganic hybrids consisting of aluminum organophos-

phonates^{6–12} and highly ordered layered structures consisting of aluminum phosphate phases separated by long alkyl chains have been obtained.^{13–18} The organic ligands may play an important role in the self-assembly pathways of the metastable species and in the change of the hydrophobicity of micropores or surfaces of aluminophosphate or aluminophosphonate materials, which in turn should affect their catalytic and sorption properties. The modification of the various forms of alumina hydroxides by reacting them with phosphoric acid mono- and diesters is claimed in several patents as an efficient method for the preparation of analytical and industrial adsorbents, flame retardants, flocculation agents, reactive fillers, etc.^{19,20} This area is, however, still in its infancy and needs new synthetic strategies and

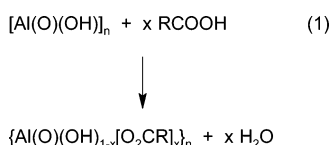
* To whom correspondence should be addressed. Fax: +48-22-660-7271. E-mail: evala@ch.pw.edu.pl

- (1) Usuki, A.; Kojima, Y.; Kawasumi, M.; Okada, A.; Fukushima, Y.; Kurauchi, T.; Kamigaito, O. *J. Mater. Res.* **1993**, *8*, 1179.
- (2) Vaia, R. A.; Hope, I.; Giannelis, E. P. *Chem. Mater.* **1993**, *5*, 1694.
- (3) Usuki, A.; Koiwai, A.; Kojima, Y.; Kawasumi, M.; Okada, A.; Kurauchi, T.; Kamigaito, O. *J. Appl. Polym. Sci.* **1995**, *55*, 119.
- (4) Vaia, R. A.; Jandt, K. D.; Kramer, E. J.; Giannelis, E. P. *Chem. Mater.* **1996**, *8*, 2628.
- (5) Vaia, R. A.; Giannelis, E. P. *Macromolecules* **1997**, *30*, 7990.

- (6) Maeda, K.; Kiyozumi, Y.; Mizukami, F. *Angew. Chem., Int. Ed. Engl.* **1994**, *33*, 2335.
- (7) Maeda, K.; Akimoto, J.; Kiyozumi, Y.; Mizukami, F. *Angew. Chem., Int. Ed. Engl.* **1995**, *34*, 1199.
- (8) Maeda, K.; Akimoto, J.; Kiyozumi, Y.; Mizukami, F. *J. Chem. Soc., Chem. Commun.* **1995**, 1033.
- (9) Maeda, K.; Hashiguchi, Y.; Kiyozumi, Y.; Mizukami, F. *Bull. Chem. Soc. Jpn.* **1997**, *70*, 345.
- (10) Kimura, T. *Chem. Mater.* **2003**, *15*, 3742.
- (11) Kimura, T. *Chem. Mater.* **2005**, *17*, 5521.
- (12) Kimura, T. *Chem. Mater.* **2005**, *17*, 337.
- (13) Fröba, M.; Tiemann, M. *Chem. Mater.* **1998**, *10*, 3475.
- (14) Tanaka, H.; Chikazawa, M. *Mater. Res. Bull.* **2000**, *35*, 75.
- (15) Schulz, M.; Tiemann, M.; Fröba, M.; Jäger, C. *J. Phys. Chem. B* **2000**, *104*, 10473.
- (16) Huang, Y.; Yan, Z. *J. Am. Chem. Soc.* **2005**, *127*, 2731.
- (17) Tiemann, M.; Fröba, M. *Chem. Mater.* **2001**, *13*, 3211.
- (18) Kimura, T. *Microporous Mesoporous Mater.* **2005**, *77*, 97.
- (19) Martin, E. S.; Wieserman, L. F. U.S. Patent 4,929,589, 1990.
- (20) Zygadło-Monikowska, E.; Florjańczyk, Z.; Wolak, A.; Lasota, A.; Plichta, A. *Polish patent application*.

fundamental studies to enable the design of desired structures and properties.

To gain a greater understanding of the interactions between aluminum species and organophosphate ligands, we have investigated the reactions of diphenylphosphoric acid (DPPA) with trialkylaluminum derivatives to obtain model compounds, the structures of which may reproduce Al–O–P phases formed during the destruction of the organized alumina core by means of phosphate ions. This includes (a) dialkylaluminum organophosphate, which may serve as the simplest isolable model of phosphate bonding to aluminum atoms, (b) polymeric materials built of aluminum diphenyl phosphate units (DPP), and (c) hybrid materials containing aluminophosphate ligands and aluminum hydroxide frameworks. We have examined these materials using elemental analysis, TGA, and several spectroscopic techniques from which useful information concerning the structure of six-coordinated aluminum phosphates has been obtained. We used also aluminum oxohydroxide [AlO(OH)] in the form of boehmite as a source of aluminum in the synthesis of aluminophosphate materials. Recent work by Barron et al. showed that the reaction of boehmite with carboxylic acids leads to the cleavage of hydrogen bonds between octahedral double layers of AlO₆ and to the replacement of hydroxyl groups by bidentate carboxylate ligands, causing exfoliation of the boehmite layers without damaging the Al–O–Al linkages.^{21,22} Therefore, the so-formed particles consist of a boehmite-like core decorated with carboxylate groups.



There are several examples of the practical application of these materials as processable precursors to α - and γ -alumina,^{22,23} nanometer-sized reactive fillers chemically incorporated into thermoset polymers^{24,25} and support for olefin polymerization catalysts.²⁶ This prompted us to check whether such kind of chemistry can be extended to the synthesis of alumoxanes modified by organophosphorus ligands.

Experimental Section

Raw Materials. The starting materials for the synthesis were as follows: DPPA (99%, Aldrich), Al(Me)₃ (2.0 M solution in toluene, Aldrich), Al(Et)₃ (1.9 M solution in toluene, Aldrich), Al(^tBu)₃ (0.8 M solution in ether, prepared according to the method described elsewhere),²⁷ and boehmite (ca. 75 wt % Al₂O₃, Catapal D Alumina,

Alta Vista Inc.). The listed materials were used as received without further purification.

Reactions of Trialkylaluminum Compounds with DPPA. In the reactions involving trialkylaluminum compounds all operations were carried out in purified nitrogen or argon atmosphere using standard Schlenk techniques. Solvents were distilled from sodium-benzophenone ketyl solution under nitrogen. A toluene solution of DPPA (0.27 M) was added dropwise to toluene or ether solutions of organoaluminum compounds that were precooled to -78 °C. The reaction mixture was allowed to warm to room temperature for 1 h. Stirring was continued for an additional 3 h. In the case of an equimolar reaction, the reaction mixture was homogeneous and a colorless viscous liquid was obtained after evaporation of the solvent under vacuum. These crude products were then dissolved in hexane and the solution was gradually cooled to -40 °C to induce the crystallization. The product of the reaction with Al(^tBu)₃ (**1**) crystallized at ca. -10 °C, whereas attempts to precipitate the crystals of analogical compounds containing methyl or ethyl groups linked to aluminum atoms failed. These compounds were hydrolyzed with water to obtain dihydroxyaluminum diphenyl phosphate (**3**). Water was added at room temperature, slowly, dropwise to the solution of the reagent in toluene, in the amount of 3 equiv of water per one aluminum atom. This resulted in the formation of a translucent gel which was dried under vacuum at 95 °C. White solid product (**2**) precipitated in the reaction systems where an excess of DPPA was used (molar ratio DPPA to AlR₃ higher than 1). The product was filtered, washed with toluene, and dried under vacuum at 50 °C. The remaining filtrate was concentrated and the thus-obtained liquid products were examined by means of spectroscopic analysis.

Reactions of Boehmite with DPPA. Boehmite (5 g, 83.3 mmol) and DPPA (62.5 g, 250 mmol) were refluxed in 200 mL of xylene for different periods of time. The resulting slurry was decanted and then centrifuged to yield a white solid material, which was purified by extraction with toluene in a Soxhlet apparatus and dried in a vacuum at 90 °C.

X-ray Structure Determination. A single crystal of **1** suitable for X-ray diffraction studies was placed in a thin walled capillary tube (Lindemann glass) in an inert atmosphere, plugged with grease, and flame-sealed. X-ray diffraction data were collected on a Nonius Kappa-CCD diffractometer. Crystal data, data collection, and refinement parameters are given in Table 1. The intensities were corrected for Lorentz-polarization effects. No absorption correction was applied. The structure was solved by direct methods using the Shelxs-97 program²⁸ and refined by the full-matrix least-squares method against F^2 values (Shelxl-97).²⁹ All non-hydrogen was refined with anisotropic displacement parameters. Difference Fourier maps indicated that one *tert*-butyl group at Al(2) shows rotational disorder about the Al–C bond over two positions. Both components are related by a rotation of $\sim 45^\circ$ about the Al(2)–C(37) bond with refined occupancy factors of 0.60(1) for major conformer. The hydrogen atoms were introduced at geometrically idealized coordinates and allowed to ride on their parent carbon atoms with assigned isotropic thermal parameters [$U_{\text{iso}} = 1.2 \times U_{\text{eq}}(\text{C})$ or $U_{\text{iso}} = 1.5 \times U_{\text{eq}}(\text{C})$ for methyl groups]. The final Fourier-difference maps have no significant chemical meaning. ORTEP drawings were made using Ortep3 for Windows.³⁰

Powder XRD Studies. Laboratory X-ray powder diffraction patterns were recorded on a Seifert HZG-4 automated diffractometer

- (21) Landry, C. C.; Pappé, N.; Mason, M. R.; Apblett, A. W.; Tyler, A. N.; MacInnes, A. N.; Barron, A. R. *J. Mater. Chem.* **1995**, *5*, 331.
 (22) Callender, R. L.; Harlan, C. J.; Shapiro, N. M.; Jones, C. D.; Callahan, D. L.; Wiesner, M. R.; MacQueen, D. B.; Cook, R.; Barron, A. R. *Chem. Mater.* **1997**, *9*, 2418.
 (23) Kareiva, A.; Harlan, C. J.; MacQueen, D. B.; Cook, R. L.; Barron, A. R. *Chem. Mater.* **1996**, *8*, 2331.
 (24) Volgelson, C. T.; Koide, Y.; Alemany, L. B.; Barron, A. R. *Chem. Mater.* **2000**, *12*, 795.
 (25) Affek, M.; Dębowski, M.; Florjańczyk, Z. *Polimery* **2003**, *48*, 528.
 (26) Obrey, S. J.; Barron, A. R. *Macromolecules* **2002**, *35*, 1499.
 (27) Lehmkuhl, H.; Olbrysh, O.; Nehl, H. *Justus Liebigs Ann. Chem.* **1973**, *708*.

- (28) Sheldrick, G. M. *SHELXS-97*, Program for Structure Solution; *Acta Crystallogr. Sect. A* **1990**, *46*, 467.
 (29) Sheldrick, G. M.; *SHELXL-97*, Program for Crystal Structure Refinement; Universität Göttingen: Göttingen, Germany, 1997.
 (30) Farrugia, L. J. *J. Appl. Crystallogr.* **1997**, *30*, 565.

Table 1. Crystal Data, Data Collection, Structure Solution, and Refinement Parameters for [(*t*Bu)₂AlO₂P(OC₆H₅)₂]₂

formula	C ₄₀ H ₅₆ Al ₂ O ₈ P ₂
formula weight, g/mol	780.85
crystal system	monoclinic
space group	<i>P</i> 2 ₁ / <i>n</i> (no. 14)
<i>a</i> , Å	12.2213(2)
<i>b</i> , Å	18.1079(2)
<i>c</i> , Å	20.3613(2)
β, deg	102.263(3)
<i>V</i> , Å ³	4403.18(11)
<i>Z</i>	4
<i>D</i> _{calc} , g·cm ⁻³	1.178
<i>F</i> (000)	1664
radiation used	Mo Kα (λ = 0.71073 Å)
μ, mm ⁻¹	0.185
θ range, deg	3.0–27.5
reflns collected	63149
unique data, <i>R</i> _{int}	10083, 0.0211
obsd data [<i>I</i> > 2σ(<i>I</i>)]	8279
data/param/restr	10083/512/0
gof on <i>F</i> ²	1.056
<i>R</i> 1, w <i>R</i> 2 (obsd data) ^a	0.0454, 0.1038
<i>R</i> 1, w <i>R</i> 2 (all data) ^a	0.0600, 0.1092
weights <i>a</i> , <i>b</i> ^b	0.0440, 2.18
largest resids, e ⁻ ·Å ⁻³	+0.34/−0.32

^a *R*1 = Σ||*F*_o| − |*F*_c||/Σ|*F*_o|, w*R*2 = [Σw(*F*_o² − *F*_c²)²/Σw(*F*_o⁴)]^{1/2}. ^b *w* = 1/[σ²(*F*_o²) + (*aP*)² + *bP*], where *P* = (*F*_o² + 2*F*_c²)/3.

using Cu Kα radiation (λ = 1.5418 Å). The data were collected in the Bragg-Brentano (θ/2θ) horizontal geometry (flat reflection mode) between 10 and 70° (2θ) in 0.04° steps, at 10 s·step⁻¹. The optics of the HZG-4 diffractometer was a system of primary Soller slits between the X-ray tube and the fixed aperture slit of 2.0 mm. One scattered-radiation slit of 2 mm was placed after the sample, followed by the detector slit of 0.2 mm.

Thermogravimetric Analysis (TGA). TGA studies were performed with a Derivatograph Q 1500-D instrument. The samples were heated under flowing dry air at a rate of 5–10 °C·min⁻¹ up to 1000 °C. TGA ceramic yield (mass loss on ignition) was used here as an alternative to chemical analysis for most of the solid products obtained.

Elemental Analysis. The hydrogen, carbon, and phosphorus contents were determined by means of a Carbo Elbo 1108 instrument. The aluminum content was determined as follows: the sample was mineralized to convert all aluminum atoms into the water-soluble form of Al³⁺, the ions were then complexed with EDTA, and the excess of EDTA was titrated with an FeCl₃ solution.

NMR and FT-IR Spectroscopies and Scanning Electron Microscopy (SEM). ¹H, ¹³C, ²⁷Al, and ³¹P NMR spectra were recorded in C₆D₆ or D₂O solutions on a Varian 400 MHz spectrometer operating at 400.11, 100.61, 104.25, and 161.96 MHz, respectively. Chemical shifts are reported relative to external [Al-(H₂O)₆]³⁺ (²⁷Al), 85% H₃PO₄ (³¹P), and TMS (¹³C and ¹H) standards. Solid-state ²⁷Al MAS NMR measurements were performed on a Bruker DSX 300 spectrometer at a spinning rate of 6–8.4 kHz with proton high-power decoupling and a resonance frequency of 78.21 MHz with a recycle time of 0.5 or 1 s. Solid-state ¹³C and ³¹P CP/MAS NMR measurements were performed at spinning rates of 8.4 and 4–8 kHz and resonance frequencies of 75.47 and 121.50 MHz with recycle times of 6 and 1 s and contact times of 1.5 and 1–1.5 ms, respectively. Processing was carried out using Bruker software, and spectra were simulated using SIMPSON.³¹

Infrared spectra were collected on a Biorad 165 FT-IR spectrophotometer with the samples in KBr pellets or in Nujol mulls between KBr plates.

(31) Bak, M.; Rasmussen, J. T.; Nielsen, N. C. *J. Magn. Reson.* **2000**, *147*, 296.

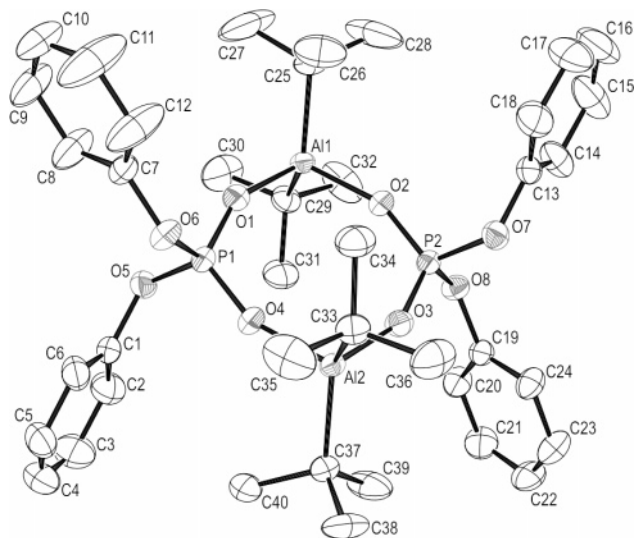
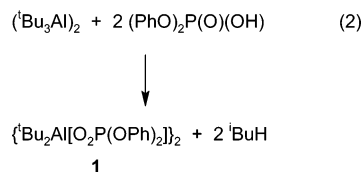


Figure 1. An ORTEP diagram of molecular structure of [(*t*Bu)₂AlO₂P(OC₆H₅)₂]₂ (**1**). Thermal ellipsoids are shown at the 50% level and hydrogen atoms are omitted for clarity.

SEM images of the powdered samples were obtained on an Hitachi S-3500N scanning electron microscope.

Results

Synthesis and Characterization of Model Aluminum Diphenyl Phosphates. *Di(tert-butyl)aluminum Diphenyl Phosphate (1).* The crystalline organoaluminum compound containing DPP ligands was obtained in the reaction of Al(*t*Bu)₃ with 1 molar equivalent of DPPA carried out in toluene. The reaction resulted in the formation of di(*tert*-butyl)aluminum diphenyl phosphate (**1**) in almost quantitative yield:



A single-crystal X-ray structure analysis revealed that in the solid state **1** exists as a dimer (Figure 1) consisting of two dialkylaluminum units bridged by two DPP ligands. The central eight-membered Al₂O₄P₂ ring is puckered (puckering amplitude *Q* = 0.4050(9) Å)³² and adopts a chairlike conformation. The four O atoms and two P atoms are close to being coplanar, while both Al atoms are substantially displaced out of this plane: −0.448(1) and 0.475(1) Å for Al(1) and Al(2), respectively. The Al···Al trans-annular separation equals 4.7505(7) Å. The aluminum atoms are in distorted tetrahedral coordination environments with bond angles ranging from about 100° (O–Al–O) to about 125° (C–Al–C).

All Al–O bond lengths are identical (within 3σ) and are in the range expected for this type of coordination.^{33,34} The

(32) Cremer, D.; Pople, J. A. *J. Am. Chem. Soc.* **1975**, *97*, 1354.

(33) Haaland, A. In *Coordination Chemistry of Aluminum*; Robinson, G. H., Ed.; VCH: New York, 1993; Chapter 1.

(34) Bethley, C. E.; Aitken, C. L.; Harlan, C. J.; Koide, Y.; Bott, S. G.; Barron, A. R. *Organometallics* **1997**, *16*, 329.

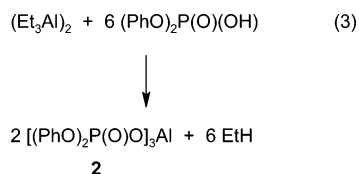
Table 2. Selected Bond Lengths (Å) and Angles (deg) for [(*t*-Bu)₂AlO₂P(OC₆H₅)₂]₂

Bond Distances			
P(1)–O(1)	1.4888(12)	Al(1)–O(1)	1.8145(12)
P(1)–O(4)	1.4880(11)	Al(1)–O(2)	1.8145(12)
P(1)–O(5)	1.5695(12)	Al(1)–C(25)	1.9750(17)
P(1)–O(6)	1.5699(12)	Al(1)–C(29)	1.9766(18)
P(2)–O(2)	1.4884(11)	Al(2)–O(3)	1.8167(12)
P(2)–O(3)	1.4872(11)	Al(2)–O(4)	1.8170(12)
P(2)–O(7)	1.5738(12)	Al(2)–C(33)	1.9754(18)
P(2)–O(8)	1.5719(11)	Al(2)–C(37)	1.9895(17)
Bond Angles			
O(1)–P(1)–O(4)	117.48(7)	O(2)–P(2)–O(3)	117.79(7)
O(1)–P(1)–O(5)	105.70(7)	O(2)–P(2)–O(7)	109.44(6)
O(1)–P(1)–O(6)	109.94(7)	O(2)–P(2)–O(8)	106.27(6)
O(4)–P(1)–O(5)	109.98(7)	O(3)–P(2)–O(7)	105.96(7)
O(4)–P(1)–O(6)	105.85(7)	O(3)–P(2)–O(8)	109.65(6)
O(5)–P(1)–O(6)	107.58(6)	O(7)–P(2)–O(8)	107.34(6)
P(1)–O(6)–C(7)	125.23(10)	P(2)–O(7)–C(13)	123.09(10)
P(1)–O(5)–C(1)	122.52(10)	P(2)–O(8)–C(19)	123.56(10)
O(1)–Al(1)–O(2)	101.75(6)	O(3)–Al(2)–O(4)	100.15(6)
C(25)–Al(1)–C(29)	125.27(8)	C(33)–Al(2)–C(37)	124.24(8)
Al(1)–O(1)–P(1)	150.33(8)	Al(2)–O(3)–P(2)	152.04(8)
Al(1)–O(2)–P(2)	156.12(8)	Al(2)–O(4)–P(1)	155.53(8)

intra-ring P–O bond distances are also indistinguishable (average 1.4881(12) Å), indicating a symmetrically bound phosphate ligand (Table 2). The overall geometry of the central (C₂Al)₂(PO₄)₂ core is similar to that found in the related cyclic dialkylaluminum phosphates.^{35–37} It should also be mentioned that phenoxy groups bonded to the P(1) atom are linked with each other by a pair of weak intramolecular C–H_{arom}···O hydrogen bonds with the aryloxy oxygen acting as a hydrogen acceptor [H(7)···O(6) 2.58 Å, C(6)–H(6)···O(6) 124° and H(8)···O(5) 2.62 Å, C(8)–H(8)···O(5) 125°]. The corresponding H···O separations for phenoxy groups of the P(2) atom are about 0.1 Å longer. The observed contacts show that the interactions are very weak; nevertheless, they influence the preferred orientation of phenyl groups.

The ¹H and ³¹P NMR spectra of **1** in C₆D₆ solutions at 25 °C display single resonances for the Al-*tert*-butyl protons at δ = 1.25 ppm and for the phosphorus nuclei at δ = –25.5 ppm, respectively. The ²⁷Al NMR spectra recorded at various concentrations at 20–50 °C showed only a very broad probe head signal that falls at about 60 ppm. The reason for this is probably the nonsymmetrical substitution of tetrahedral aluminum nuclei in **1** which results in a very short relaxation time.

Aluminum Tris(diphenyl phosphate) (2). The title compound has been synthesized in the reaction of 3 equiv of DPPA with Et₃Al in toluene at ambient temperature:



(35) Mason, M. R.; Matthews, R. M.; Mashuta, M. S.; Richardson, J. F. *Inorg. Chem.* **1996**, *35*, 5756.

(36) Pinkas, J.; Chakraborty, D.; Yang, Y.; Murugavel, R.; Noltemeyer, M.; Roesky, H. W. *Organometallics* **1999**, *18*, 523.

(37) Lugmair, C. G.; Tilley, T. D.; Rheinhold, A. L. *Chem. Mater.* **1999**, *11*, 1615.

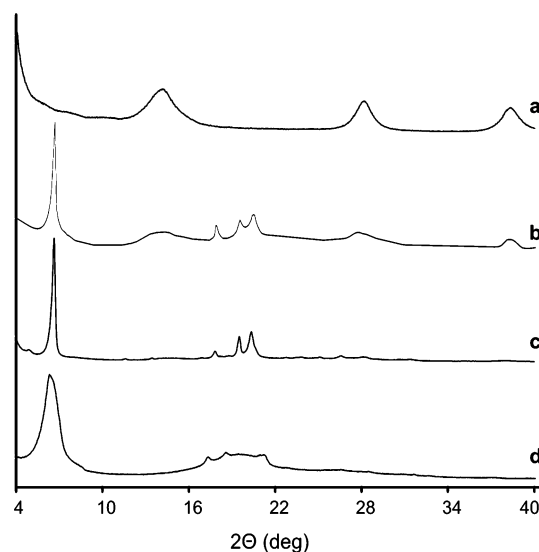


Figure 2. X-ray powder diffraction pattern of (a) boehmite, (b) product of the reaction of DPPA and boehmite after 6 h, (c) product of the reaction of DPPA and boehmite after 48 h, and (d) **2**.

The elemental analysis of precipitated white solid, which is insoluble in water and in common organic solvents, corresponds fairly well with the calculated composition for compound **2**. (Calculated for C₃₆H₃₀AlP₃O₁₂: C, 55.82%; H, 3.90%; Al, 3.48%; P, 12.00%. Found: C, 55.2%; H, 3.7%; Al, 3.3%; P, 12.5%). The ¹³C MAS NMR spectrum, which shows only four signals of phenyl group resonance at 119.3, 122.1, 128.8, and 151.5 ppm, also supports the proposal that alkyl groups are completely removed from the aluminum atoms. The ceramic yield determined by means of TGA (24.9%) is equal to the theoretical value for the inorganic residue Al₂O₃·2P₂O₅. The decomposition starts at about 200 °C and the main mass loss of ca. 61% occurs in the temperature range 300–450 °C.

The X-ray powder diffraction pattern of **2** (Figure 2d) points out the very low crystallinity of this material. The strongest reflection at 2θ = 6.36° with a *d* spacing distance of 13.9 Å might suggest a kind of layered or fibrous arrangement of molecules. The set of weaker reflections occurs in the range from 17 to 23°.

The ²⁷Al MAS NMR spectrum (Figure 3a) of **2** shows a single resonance (*W*_{1/2} ~ 600 Hz) at δ = –23.2 ppm that can be attributed to the six-coordinated Al nuclei. The peak position is reasonable for an octahedral aluminum, when compared for example with those of crystalline α-, β-, and ζ-aluminum methylphosphonate (δ = –21.3, –17.5, and –18.5 ppm, respectively)^{6–9} and six-coordinate aluminum in natural or synthetic hydrated aluminum phosphates.^{38,39}

In contrast, the ³¹P MAS NMR spectrum (Figure 4a) exhibits three signals (accompanied by several spinning sidebands) which can be related to the unequivalent P sites attached to AlO₆ units. The observed chemical shifts at ca. –9, –16, and –24 ppm occur in the range characteristic of tetrahedral phosphorus in aluminum phosphates of layered or network structures.^{15,35}

The FT-IR spectrum of **2** (Figure 5b) reveals three strong signals that may be attributed to the stretching vibrations of

(38) Blackwell, C. S.; Patton, R. L. *J. Phys. Chem.* **1984**, *88*, 6135.

(39) Blackwell, C. S.; Patton, R. L. *J. Phys. Chem.* **1988**, *92*, 3965.

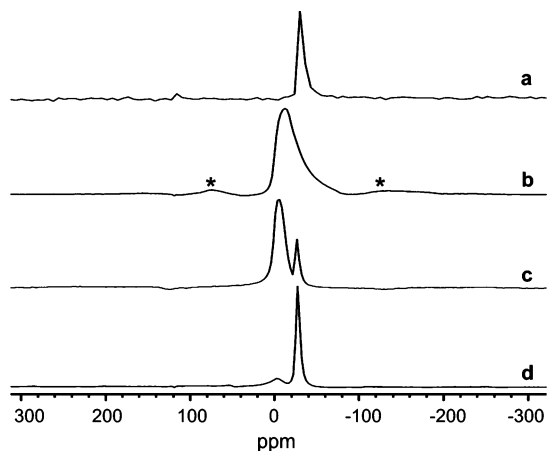


Figure 3. ^{27}Al MAS NMR spectra of (a) **2**, (b) **3**, (c) the product of the reaction of DPPA with boehmite after 6 h, and (d) the product of the reaction of DPPA with boehmite after 48 h. Asterisks depict spinning sidebands.

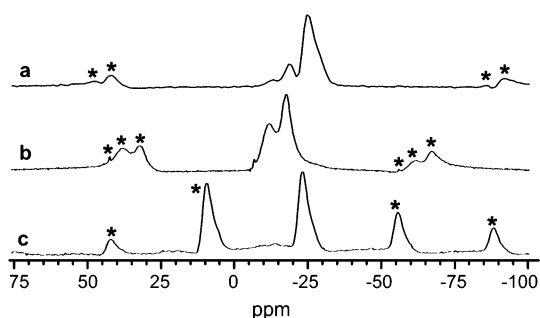


Figure 4. ^{31}P MAS NMR spectra of (a) **2**, (b) **3**, and (c) the product of the reaction of DPPA and boehmite after 48 h. Asterisks depict spinning sidebands.

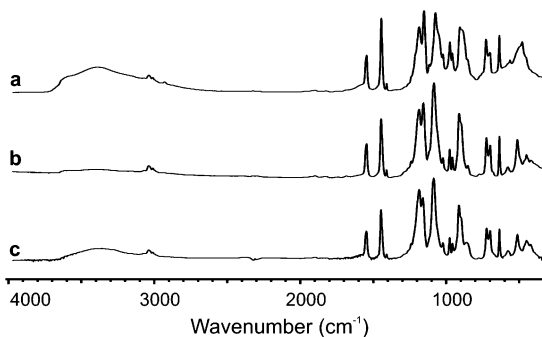
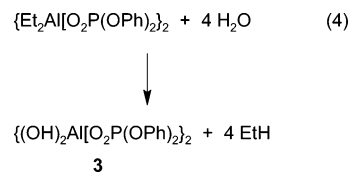


Figure 5. FT-IR spectra of (a) **3**, (b) **2**, and (c) the product of the reaction of DPPA and boehmite after 48 h.

P—O bonds in the bridging units at 1233, 1203, and 1133 cm^{-1} . Due to the conjugation of the vibrations of four P—O bonds (two bonds from the Al—O—P—O—Al bridge and two terminal P—O—C bonds) and to the lack of information on the ligands geometry, it is not possible to precisely attribute those peaks to specified types of vibrations. Based on the literature data for FT-IR spectra of well-defined aluminum derivatives of phosphinic acids, it can be supposed that the band for the symmetric stretching vibrations in Al—O—P—O—Al bridges occurs at ca. 1100 cm^{-1} while the appropriate band for the asymmetric vibrations occurs in the range of 1150–1200 cm^{-1} .⁴⁰

Dihydroxyaluminum Diphenyl phosphate (3). To obtain the materials with structures reproducing the bonding features

of hybrid polymers containing Al—O—P—O—Al and Al—O—H units, the equimolar reaction of AlEt_3 with DPPA was carried out and next the reaction products were hydrolyzed. It was expected that salt **3** will be the main product of the hydrolysis:



The reaction was carried out in toluene at room temperature and the hydrolysis product precipitated as a white powder under these conditions. The elemental analysis of the product dried under vacuum at 90 °C shows that the composition is not homogeneous. The mean carbon, hydrogen, and aluminum contents are equal to ca. 45.0%, 4.0%, and 8.7%, respectively. These values are similar to those calculated for **3** (C, 46.4%; H, 3.9%; Al, 8.7%) and the observed differences are probably the result of the small amounts of adsorbed water molecules. The TGA analysis of the hydrolyzate reveals that the sample loses 1–4% of its weight before the temperature reaches 130 °C, due to the removal of the adsorbed water. At higher temperatures phenol constitutes the main volatile product. The highest weight loss (ca. 33%) is observed in the range of 200–300 °C and one may attribute it to the elimination of one molecule of phenol from **3**. The total weight loss in the range of 120–1000 °C is equal to ca. 58%, which is in reasonable agreement with the ceramic yield for the decomposition of **3** to AlPO_4 , which is calculated to be 39.4%.

The FT-IR spectrum of **3** (Figure 5a) exhibits a broad band assigned to the stretching vibrations of O—H groups at ca. 3600 cm^{-1} . The majority of the remaining signals has similar positions to those presented in the spectrum of **2** (Figure 5b). The important difference between both spectra occurs at ca. 1100 and 550 cm^{-1} in the regions characteristic of the P—O stretching vibrations and the Al—O skeleton vibrations, respectively. The signals of the P—O stretching vibrations in **3** appear at 1235, 1201, and 1124 cm^{-1} . In the spectrum of sample **3** subjected to high temperature (200–220 °C) to remove organic groups (not shown here), a number of new, intense signals appear in the range of 1050–1200 cm^{-1} at the expense of the peak at 1235 cm^{-1} . We suggest, therefore, that the main contribution to this last peak comes from P—OC₆H₅ vibrations, whereas the signals at about 1200 and 1120–1130 cm^{-1} in aluminum diphenyl phosphates can be attributed to asymmetric and symmetric stretches in the Al—O—P—O—Al bridges. The ^{31}P MAS NMR spectrum of **3** (Figure 4b) indicates the presence of several different types of ligands. Deconvolution of the spectrum (see Supporting Information) suggests that there are four kinds of nonequivalent DPP environments which correspond to signals at ca. -27, -18, -12, and -7 ppm. The ^{27}Al MAS NMR spectrum of **3** (Figure 3b) shows a broad signal ($W_{1/2} \sim 2300$ Hz) of the six-coordinated aluminum nuclei, centered at ca. -9 ppm.

Reaction of Boehmite with DPPA. Powdered boehmite refluxed in the air atmosphere with an excess of DPPA

(40) Olapinski, H.; Schaible, B.; Weidlein, J. *J. Organomet. Chem.* **1972**, *43*, 107.

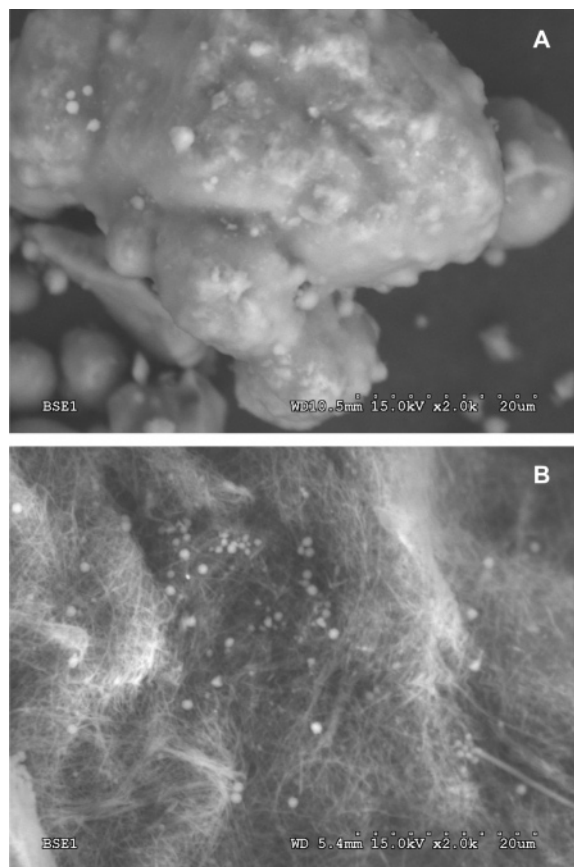
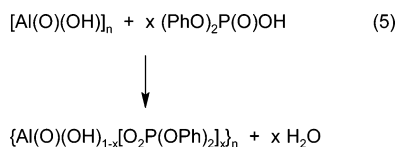


Figure 6. SEM images of (a) boehmite and (b) the product of the reaction of DPPA and boehmite after 48 h.

dissolved in xylene results in the formation of Al–O–P phase:



In the FT-IR spectra of the thus-obtained products, a decrease in the intensity of signals characteristic of O–H groups (O–H stretching vibrations: ν_{as} at 3305 cm^{-1} and ν_{s} at 3072 cm^{-1} ; O–H bending vibrations: δ_{as} at 1157 cm^{-1} , δ_{s} at 1072 cm^{-1} , and γ at 737 cm^{-1}) and distorted AlO_6 octahedrons (Al–O stretching vibrations: ν at 674 , 615 , and 475 cm^{-1}) in the boehmite structure as well as the appearance of a rich spectrum typical for DPP anions can be observed (main signals: 1234 , 1210 , and 1135 cm^{-1}).⁴¹ After ca. 48 h of reaction, the FT-IR spectrum of the product (Figure 5c) is similar to that of **2**, with additional small broad signals attributable to stretching vibrations of O–H groups at ca. 3400 cm^{-1} , and prolongation of the reaction time does not result in significant changes. The samples of this material examined by SEM were found to consist of irregular agglomerates, which at higher magnification reveal a fibrous structure with a particle size to be less than 100 nm in diameter (Figure 6b) and small spherical particles varying in size from 0.5 to 1.5 μm in diameter. This kind of

(41) Kiss, A. B.; Keresztury, G.; Farkas, L. *Spectrochim. Acta, Part A* **1980**, *36*, 653.

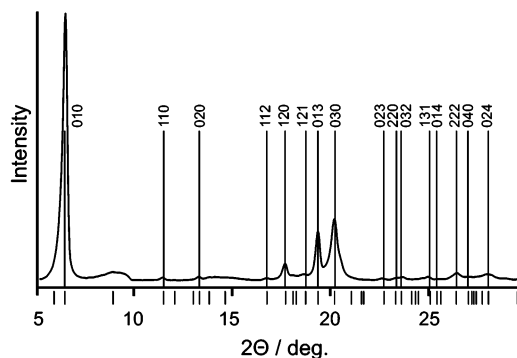


Figure 7. XRD pattern of the product of reaction of DPPA and boehmite. The calculated Bragg reflections are shown under the axis.

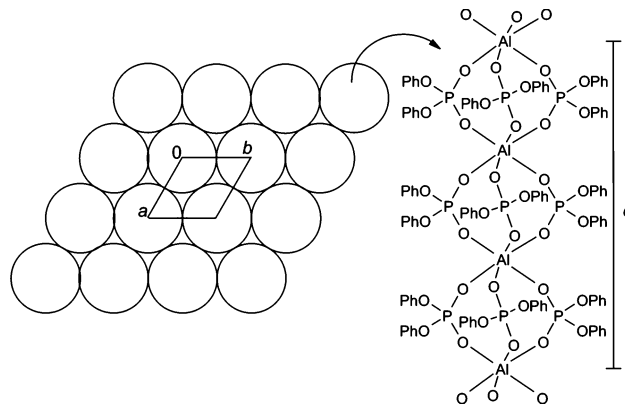


Figure 8. Schematic representation of the structural model of catena-Al-(DPP)₃.

morphology was not observed either for boehmite as the starting material (Figure 6a) or for the samples of compounds **2** and **3**, which exist as solid agglomerates composed of small particles packed together.

Apart from the broad and weak reflections attributable to the residual crystalline boehmite structure (Figure 2a) which can be detected in the XRD patterns of these products (Figures 2b and 2c), the new strong reflection at $6.7^\circ 2\theta$ ($d = 13.2 \text{ \AA}$) and the set of less intense reflections in the range of $11\text{--}30^\circ 2\theta$ appear. Based on these reflections, an attempt of indexing the XRD pattern was undertaken. Good matching was obtained for the hexagonal system with the unit cell parameters $a = 15.14(4) \text{ \AA}$ and $c = 14.44(3) \text{ \AA}$ ($V = 2870 \text{ \AA}^3$). The so-called F_{16} figure of merit was equal to 10.9 (0.042, 35).⁴² The calculated Bragg reflection positions are presented in Figure 7.

These results allowed us to suggest that the product of the reaction of DPPA and boehmite bears a fibrous structure consisting of polymeric chains of catena-Al(DPP)₃. In our opinion the polymer consists of repeating units containing octahedrally coordinated Al atoms bridged by three DPP ligands forming the polymer chain which propagates along the c direction of the unit cell. The large diffraction peak at $2\theta = 6.7^\circ$ in the XRD pattern is due to the chains arranged in the form of a close-packed hexagonal columnar structure as was depicted in Figure 8. Assuming that the mean volume of each non-hydrogen atom in the structure should be close to 20 \AA^3 (i.e., the volume of the Al(DPP)_3 molecule ≈ 1000

(42) Smith, G. S.; Snyder, R. L. *J. Appl. Crystallogr.* **1979**, *12*, 60.

\AA^3), the number of molecules of $\text{Al}(\text{DPP})_3$ in the crystallographic unit cell (Z) is 3. Therefore, the mean diameter of the chain should be equal to the parameter α (15.14 \AA), while the distance between adjacent Al atoms linked by three phosphate bridges can be estimated as $c/3 = 4.81 \text{ \AA}$. The latter value matches perfectly with the value of the $\text{Al}\cdots\text{Al}$ separation determined for compound **1** [4.7505(7) \AA]. Moreover, the diameter of the chain is comparable to the estimated dimension (ca. 14 \AA) of the trinuclear linear vanadium–magnesium complex $[\text{LV}(\mu_2\text{-DPP})_3]_2\text{Mg}$ (L = hydrotris(pyrazolyl)borate) comprising a central octahedral magnesium cation facially coordinated on either side by a $\text{LV}(\text{DPP})_3^-$ moiety.⁴³

The ^{31}P MAS NMR spectrum (Figure 4c) shows a strong, quite narrow (ca. 500 Hz) but not fully symmetrical signal at -24 ppm and a weak, broad signal at ca. -13 ppm (both of them are accompanied by several spinning sidebands). The deconvolution of the spectra (see Supporting Information) shows, however, that the main peak consists of two signals at ca. -24 and -26 ppm. This suggests that only part of the bridging DPP units forms the catena- $\text{Al}(\text{DPP})_3$ structure while the other ones belong to another phase.

The ^{27}Al MAS NMR spectra (Figures 3c and 3d) exhibit two signals attributable to six-coordinated Al nuclei. The broad signal ($W_{1/2} \sim 1200$ Hz) centered at ca. -2 ppm has a similar chemical shift to that of boehmite ($\delta_{\text{Al}} \sim -3$ ppm). The second signal at about -23 ppm ($W_{1/2} \sim 500$ Hz) is attributed to the Al nuclei in Al–O–P phases (the chemical shift of the signal is similar to those for Al nuclei in **2**). The relative intensity of this signal increases at the expense of the broad peak with the advancement of the reaction time, accounting for 50–55% of total aluminum in the product with the highest content of DPP ligands.

The attempts to obtain self-consistent elemental analysis for these products failed. The carbon and hydrogen analysis varied slightly between the samples within a reaction run; however, higher differences in the aluminum and phosphorus contents were observed. After a long reaction time the maximum C content in the product is equal to 47.7–48.0%, the maximum H content is approximately 3.6–3.8%, and that of Al is 5.8–6.5%. This suggests that DPP ligands constitute ca. 83% of the total mass and that the average number of DPP per one Al atom is higher than 1 (1.4–1.5). The TGA analysis indicates that the samples contain 1.5–2% of adsorbed water which is being removed at a temperature lower than 200 $^\circ\text{C}$. The total weight loss in the range of 200–1000 $^\circ\text{C}$ is equal to 61.0%. The ^{27}Al MAS NMR spectrum of the calcined product shows that six-coordinated aluminum species in the aluminum phosphate phase have been converted to the tetrahedral site $\text{Al}(\text{-OP})_4$, giving rise to a sharp signal at 31 ppm. The spectrum contains also a broad signal at about -5 ppm that can be attributed to the AlO_6 phase.

Based on all the experimental data collected, it is supposed that the reaction of boehmite with DPPA leads to a mixture

of products containing both an alumoxane and aluminophosphate core.

Discussion

An eight-membered $\text{Al}_2\text{O}_4\text{P}_2$ ring present in **1** is probably a common structural feature of dialkylaluminum phosphates^{35–37,44} and many other four-coordinated aluminum clusters containing phosphate, phosphonate, or phosphinate ligands.^{44,45} The absence of ligands chelating to one metal atom is attributed to the steric strain that would be present in the four-membered AlPO_2 ring.⁴⁶ In the reactions of $\text{Al}(\text{Me})_3$ and $\text{Al}(\text{Et})_3$ with DPPA no stable cyclic dialkylaluminum diphenyl phosphates are formed. Viscous oil-like products are obtained when the reagents are used in equimolar amounts. The mean molecular weights determined by means of the cryoscopic method (for the just-obtained products in benzene solutions) were equal to ca. 580 and ca. 650 $\text{g}\cdot\text{mol}^{-1}$ for methyl and ethyl derivatives, respectively. These values are close to theoretical molecular weights of the dimers of dialkylaluminum diphenyl phosphates which are equal to 612 and 668 $\text{g}\cdot\text{mol}^{-1}$, respectively. After a few weeks, **2** precipitates from the solutions described above. Moreover, after that time weak signals attributable to six-coordinated Al nuclei at ca. 0 and ca. -20 ppm in the ^{27}Al NMR spectra of the solutions and two or three signals in the range of -25 to -26.5 ppm in the ^{31}P NMR spectra of the solutions may be observed. Both these facts indicate that the process of the ligands interchange occurs in the systems where alkyl groups are too small to cause any steric hindrance. This process is accelerated by the substitution of the second alkyl group at the aluminum center and compound **2** precipitates from the reaction system immediately when the molar ratio of DPPA to trialkylaluminum is slightly higher than 1.

The XRD pattern of **2** indicates that aluminum tris(diphenyl phosphate) obtained from organometallic precursors is poorly crystallized and, therefore, the exact structure of this material cannot be solved. It is interesting to note that all Al atoms in the aluminum phosphate phase formed herein possess an octahedral AlO_6 coordination, despite a large steric hindrance introduced by DPP ligands. For this type of coordination the number of P atoms in the second coordination sphere theoretically may vary from 3 to 6, depending on the mode of DPP coordination.

The ^{31}P NMR MAS spectrum of **2** reveals the existence of the P sites in three nonequivalent environments. The theoretical study for a series of phosphates indicates that the shielding tensor is not directly related to the bonding electron distribution and the paramagnetic contribution is rather dominant in the determination of chemical shifts in ^{31}P MAS NMR spectra.⁴⁷ Several empirical attempts show, however, that there is a roughly linear empirical relationship between

(43) Dean, N. S.; Mokry, L. M.; Bond, M. R.; Mohan, M.; Otieno, T.; O'Connor, C. J.; Spartalian, K.; Carrano, C. J. *Inorg. Chem.* **1997**, *36*, 1424.

(44) Mason, M. R. *J. Cluster Sci.* **1998**, *9*, 1.

(45) Walawalker, M. G.; Roesky, H. W.; Murugavel, R. *Acc. Chem. Res.* **1999**, *32*, 117.

(46) Karayannis, N. M.; Mikulski, C. M.; Pytlewski, L. L. *Inorg. Chim. Acta Rev.* **1971**, *5*, 69.

(47) Prado, F. R.; Giessner-Prettre, C.; Pullman, B.; Daudey J. P. *J. Am. Chem. Soc.* **1979**, *101*, 1737.

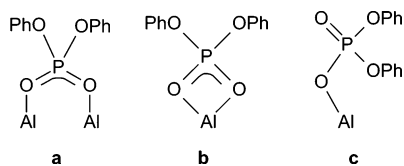


Figure 9. Modes of DPP coordination: (a) bidentate bridging ligand, (b) bidentate chelating ligand, and (c) monodentate ligand.

isotropic ^{31}P chemical shifts observed in the solid state and the mean values of P–O bond lengths⁴⁷ or P–O–P and Al–O–P angles.^{9,48} Therefore, we suggest that the strongest signal in the ^{31}P MAS NMR spectrum of **2** at -24 ppm corresponds to the bridging DPP ligands (Figure 9a) of the geometrical parameters close to that in compound **1**, which exhibit the resonance at -25.5 ppm. Two other signals observed in the spectrum of **2** at δ ca. -11 and -18 ppm can be assigned to ligands in which the mean P–O–Al bond angle is significantly lower than that in **1**. The origin of these resonances is not clear. They may come from chelating (Figure 9b) or monodentate (Figure 9c) terminal ligands disturbing the self-organization of aluminophosphate chains containing $\text{Al}(\text{OP})_6$ building blocks linked by DPP bridging ligands.

The products of the reaction of DPPA and boehmite contain a significantly lower number of these defects, which explains why $\text{Al}(\text{OP})_6$ units form quasi-regular fibrous structures similar to that of $[\text{Al}(\text{H}_2\text{PO}_4)_3]$ chains described by Kniep and Steffen.⁴⁹ The octahedral $\text{Al}(\text{OP})_6$ environment is, however, extremely rare in crystalline aluminophosphates. The quasi-perfect $\text{Al}(\text{OP})_6$ octahedral units located inside the aluminophosphate sheets built up mainly from alternating P and Al tetrahedra has been recently found to exist in the two-dimensional layered aluminophosphate templated by 1,8-diaminooctane molecules. Tuel et al. reported that the shift of such Al sites is about -19 ppm.⁵⁰ On the other hand, an analysis of accessible structural data for the complexes of trivalent cations containing an octahedral coordination center and bridging dialkyl phosphate-*O,O'* ligands showed that polymeric chain structures with triple bridges are common for diethyl phosphate derivatives of the lanthanides Ce, Pr,⁵¹ and Nd.⁵² These chains show almost hexagonal packing in the solid state, while their diameter is equal to ca. 12 \AA . Moreover, it has been found that organically modified zinc phosphates may form chain structures as well, where Zn atoms are linked to each other by one or three di(*tert*-butyl)-phosphate bridges alternatively.⁵³ Therefore, it can be concluded that organic ligands derived from phosphoric acid diesters tend to form triple bridge metal centers in chain-building units of higher dimensionality structures.

Based on the relative intensity of signals in the ^{27}Al MAS NMR spectrum, one may estimate that, in the case of the

long-time reaction run, ca. 50% of Al atoms in the product of the reaction of DPPA and boehmite exists as $\text{Al}(\text{OP})_6$ phase, while the remaining Al atoms keep the Al_2O_3 scaffold. These products were separated by hydrothermal treatment at 140°C , which resulted in the formation of two solid phases which differ in density. The density of the phase which contains more than 70% of $\text{Al}(\text{PO})_6$ units is lower than that of water, while the alumoxane-rich phase accumulates on the reaction vessel bottom. $\text{AlO}_4(\text{OH})_x(\text{OP})_{2-x}$ is expected to be the general chemical environment at Al sites in alumoxane domains; however, ^{27}Al MAS NMR spectra give no indication on the actual number of DPP ligands attached to the Al site. In our opinion, the content of DPP ligands in these structures is rather small due to the fact that over the whole sample the average number of DPP ligands per one Al atom is equal to 1.4–1.5 and in the case of the $\text{Al}(\text{OP})_6$ phase this ratio is equal to 3. The XRD pattern indicates, however, that only traces of the original crystalline boehmite structure are present in the final product. This phase is located probably inside the spherical nanoparticles (observed in SEM micrograph) that remain after gradual removal of external layers of starting material under the action of DPPA. The remaining part of the alumoxane structures is incorporated in the aluminum phosphate phase.

These observations bring us to the conclusion that, contrary to the reaction with carboxylic acids, selective substitution of hydroxyl groups in boehmite particles (see eq 1) as the effect of the reaction of boehmite with phosphoric acid diesters is impossible because the Al_2O_3 volume is too small to allow the organic groups to be linked to every Al atom (see Supporting Information where simple model calculations are shown).

Probably due to this, attempts to obtain diphenyl phosphate-alumoxane by condensation of **3** have failed. In this case the sol–gel methodology (a “bottom-up” approach) leads to the elimination of phenol instead of water molecules.

Conclusion

We have determined that the reaction of DPPA with trialkylaluminum compounds or boehmite affords the formation of the aluminophosphate phase which is built of octahedral Al atoms linked to six P atoms via oxygen bridges and thus forming $\text{Al}(\text{PO})_6$ units. The tetracoordinated aluminum phosphates obtained in the reaction with trialkylaluminum compounds are probably the transition products in the synthesis of that phase and the small molecular model containing DPP bridges (**1**) has been isolated and characterized. Based on the spectroscopic data, we claim that the similar type of bridging bonds that occur in **2** and in the products of the reaction of DPPA and boehmite does not occur in **3** where Al atoms may additionally form bridges via the hydroxyl group.

The reaction of boehmite with DPPA leads to two populations of products. One of them consists of spherical nanoparticles which we believe maintain the boehmite core decorated with aluminophosphates. The other is built of highly crystalline fibrous structures containing $\text{Al}(\text{PO})_6$ chains doped with small amounts of incorporated Al–O–Al linkages. Both types of products seem to be interesting

(48) Müller, D.; Jahn, E.; Ladwig, G.; Haubenreisser, U. *Chem. Phys. Lett.* **1984**, *109*, 332.

(49) Kniep, R.; Steffen, M. *Angew. Chem., Int. Ed. Engl.* **1978**, *17*, 272.

(50) Tuel, A.; Gramlich, V.; Baerlocher, C. *Microporous Mesoporous Mater.* **2001**, *47*, 217.

(51) Han, Y.; Pan, Z.; Shi, N.; Liao, L.; Liu, C.; Wu, G.; Tang, Z.; Xiao, Y. *Wuji Huaxue Xuebao (Chin. J. Inorg. Chem.)* **1990**, *6*, 17.

(52) Lebedev, V. G.; Palkina, K. K.; Maksimova, S. I.; Lebedeva, E. N.; Galaktionova, O. V. *Zh. Neorg. Khim.* **1982**, *27*, 2980.

(53) Lugmair, C. G.; Tilley, T. D.; Rheingold, A. L. *Chem. Mater.* **1997**, *9*, 339.

candidates for practical application in polymer composites providing that one can effectively separate them. We have found that in some systems the separation can be easily done by appropriate hydrothermal treatment which leads to the formation of two phases: the stable dispersion of spheric nanoparticles (30–60 nm) and fibers precipitating from the reaction mixture.²⁰ The method of separation of both phases as well as their chemical and morphological characterization will be described in a forthcoming paper.⁵⁴ Another aim of future work is to apply this methodology to the synthesis of functional hybrid aluminophosphate and to find the relation between the structure of organic ligands and the mode of the organization of the inorganic core.

(54) Florjańczyk, Z. In preparation.

Acknowledgment. The authors would like to gratefully acknowledge the support of the Polish State Committee for Scientific Research (4 T09B 001 25; 2003-2006). Thanks are also due to Jeffrey Fenton and CONDEA-Vista Company for complimentary delivery of boehmite samples.

Supporting Information Available: Crystallographic information on **1**; TGA curves of **2** and **3** and of the product of the reaction between DPPA and boehmite; discussion on model calculations for the product of the reaction between DPPA and boehmite; fitted ³¹P MAS NMR spectra of **3** and of the product of the reaction between DPPA and boehmite. This material is available free of charge via the Internet at <http://pubs.acs.org>.

CM0526718